

**This is a self-archived version of an original article. This version may differ from the original in pagination and typographic details.**

**Author(s):** Klee, Jan L.; Kiliaan, Amanda J.; Lipponen, Arto; Battaglia, Francesco P.

**Title:** Reduced firing rates of pyramidal cells in the frontal cortex of APP/PS1 can be restored by acute treatment with levetiracetam

**Year:** 2020

**Version:** Accepted version (Final draft)

**Copyright:** © 2020 Elsevier

**Rights:** CC BY-NC-ND 4.0

**Rights url:** <https://creativecommons.org/licenses/by-nc-nd/4.0/>

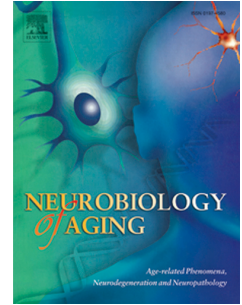
**Please cite the original version:**

Klee, J. L., Kiliaan, A. J., Lipponen, A., & Battaglia, F. P. (2020). Reduced firing rates of pyramidal cells in the frontal cortex of APP/PS1 can be restored by acute treatment with levetiracetam. *Neurobiology of Aging*, 96, 79-86. <https://doi.org/10.1016/j.neurobiolaging.2020.08.013>

# Journal Pre-proof

Reduced firing rates of pyramidal cells in the frontal cortex of APP/PS1 can be restored by acute treatment with levetiracetam

Jan L. Klee, Amanda J. Kiliaan, Arto Lipponen, Francesco P. Battaglia



PII: S0197-4580(20)30269-4

DOI: <https://doi.org/10.1016/j.neurobiolaging.2020.08.013>

Reference: NBA 10929

To appear in: *Neurobiology of Aging*

Received Date: 18 August 2019

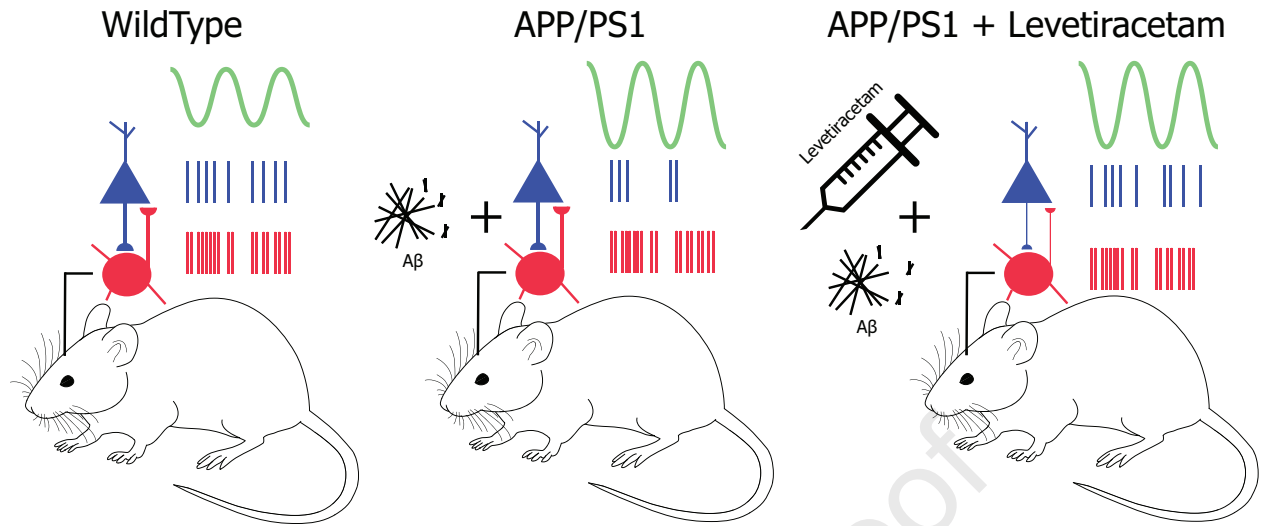
Revised Date: 3 August 2020

Accepted Date: 19 August 2020

Please cite this article as: Klee, J.L., Kiliaan, A.J., Lipponen, A., Battaglia, F.P., Reduced firing rates of pyramidal cells in the frontal cortex of APP/PS1 can be restored by acute treatment with levetiracetam, *Neurobiology of Aging* (2020), doi: <https://doi.org/10.1016/j.neurobiolaging.2020.08.013>.

This is a PDF file of an article that has undergone enhancements after acceptance, such as the addition of a cover page and metadata, and formatting for readability, but it is not yet the definitive version of record. This version will undergo additional copyediting, typesetting and review before it is published in its final form, but we are providing this version to give early visibility of the article. Please note that, during the production process, errors may be discovered which could affect the content, and all legal disclaimers that apply to the journal pertain.

© 2020 Published by Elsevier Inc.



1 Primary research article

2

3 **Reduced firing rates of pyramidal cells in the frontal cortex of APP/PS1 can be restored by**  
4 **acute treatment with levetiracetam**

5

6 Jan L. Klee<sup>1</sup>, Amanda J. Kiliaan<sup>2</sup>, Arto Lipponen<sup>3\*</sup>, Francesco P. Battaglia<sup>1\*</sup>

7 1) Department of Neuroinformatics, Radboud University, Nijmegen, the Netherlands

8 2) Department of Anatomy, Donders Institute for Brain, Cognition, and Behaviour,  
9 Radboud university medical center, Nijmegen, the Netherlands

10 3) Department of Psychology, University of Jyväskylä, Finland

11 \* equal contribution

12 Corresponding author

13 Email Arto.Lipponen@jyu.fi

14 Tel +358407169558

15 P.O. Box 35

16 FIN-40014 University of Jyväskylä

17 Jyväskylä, Finland

18 The authors report no conflicts of interest.

19 Keywords: amyloid, local field potential (LFP), single cell, firing rate, mouse model,  
20 Alzheimer's disease

21

22

23

24

25

26

27 *Highlights*

28 - 9 months old APP/PS1 mice exhibit increased theta and beta oscillations in the frontal  
29 cortex

30 - Pyramidal cell firing rates are significantly decreased but more phase-locked to ongoing LFP  
31 oscillations

32 - Levetiracetam treatment uncouples pyramidal cells and interneurons and elevates  
33 pyramidal cell firing rates

34

35

36 *Abstract*

37

38 In recent years aberrant neural oscillations in various cortical areas have emerged as a  
39 common physiological hallmark across mouse models of amyloid pathology and patients  
40 with Alzheimer's disease. However, much less is known about the underlying effect of  
41 amyloid pathology on single cell activity. Here, we used high density silicon probe recordings  
42 from frontal cortex area of 9 months old APP/PS1 mice to show that Local Field Potential  
43 (LFP) power in the theta and beta band is increased in transgenic animals, while single cell  
44 firing rates, specifically of putative pyramidal cells, are significantly reduced. At the same  
45 time, these sparsely firing pyramidal cells phase-lock their spiking activity more strongly to  
46 the ongoing theta and beta rhythms. Furthermore, we demonstrated that the anti-epileptic  
47 drug, levetiracetam, counteracts these effects by increasing pyramidal cell firing rates in  
48 APP/PS1 mice and uncoupling pyramidal cells and interneurons. Overall, our results highlight  
49 reduced firing rates of cortical pyramidal cells as a pathophysiological phenotype in APP/PS1  
50 mice and indicate a potentially beneficial effect of acute levetiracetam treatment.

51

52

53

54

55

56

57

58

59

60

61 *1. Introduction*

62

63 Network hyper-synchrony and altered neural oscillation have been suggested to contribute  
64 to the pathophysiology of Alzheimer's disease (AD) and to the accumulation of AD related  
65 amyloid protein (Busche and Konnerth, 2015; Hardy and Selkoe, 2002; Joutsa et al., 2017;  
66 Palop and Mucke, 2016). A better understanding of altered neural oscillations in AD could,  
67 therefore, provide a target for pharmacological interventions. Even though amyloid plaques  
68 and related neuronal loss are among the most significant findings in the post mortem brain  
69 of AD patients, the amount of plaques does not correlate with the severity of dementia  
70 (Nagy et al., 1995), and the removal of plaques does not lead to an improvement of memory  
71 (Holmes et al., 2008). Intriguingly, amyloid accumulation seems to cause excitatory-  
72 inhibitory imbalance at the synaptic level, triggering abnormal patterns at both the single  
73 cell and network levels which manifest as epileptiform discharges (Minkeviciene et al.,  
74 2009). Simultaneously with amyloid plaque formation, both hyper- and hypoactive neurons  
75 emerge in the hippocampus and cortical areas (Busche et al., 2012, 2008). Less is known  
76 about which subpopulations of cells are affected by amyloid accumulation but it has been  
77 proposed that this pathological process is related to persistently decreased resting  
78 membrane potential in neocortical pyramidal neurons (Minkeviciene et al., 2009). Similarly,  
79 it has been reported that basic biophysical properties of pyramidal neurons in the frontal  
80 cortex are intact but external stimulation of these neurons revealed hyper-excitability,  
81 indicating a combination of both intrinsic electrical and extrinsic synaptic dysfunctions as  
82 mechanisms for activity changes (Kellner et al., 2014). Importantly, aberrant excitatory  
83 activity in AD mouse models has also been found to result in a compensatory strengthening  
84 of inhibitory circuits which could lead to an overall suppression of neural activity (Palop et  
85 al., 2007). Whether these findings apply to in vivo unanesthetized mice, needs to be verified.

86

87 On the level of neuronal assemblies, the most prominent finding related to amyloid  
88 pathology is abnormally high Local Field Potential (LFP) power over a broad frequency range  
89 and during a wide variety of behavioral states (Goutagny et al., 2013; Gurevicius et al., 2013;  
90 Jin et al., 2018; Pena-Ortega et al., 2012; Verret et al., 2012), which can lead to epileptiform

91 synchronous discharges and generalized seizure activity (Gurevicius et al., 2013; Jin et al.,  
92 2018; Lam et al., 2017; Minkeviciene et al., 2009; Palop and Mucke, 2016; Vossel et al.,  
93 2013). The mechanism by which aberrant single cell activity changes into the generalized  
94 epileptiform activity of neuronal ensembles is not clear. Traditionally, epileptic seizures have  
95 been characterized as hypersynchrony of large neuronal populations leading to the  
96 epileptiform state (Jiruska et al., 2013). However, this view has been challenged by the  
97 finding that, during epileptic seizures, there are both increases and decreases in firing rates  
98 of neurons, many neurons are unchanged and increased tonic GABAergic inhibition is  
99 commonly found in absence epilepsy (Cope et al., 2009; Schevon et al., 2012; Truccolo et al.,  
100 2011; Wyler et al., 1982). Furthermore, single cell activity outside the periods of seizures  
101 and areas of epileptic foci is more heterogeneous and unsynchronized, and not well  
102 characterized (Keller et al., 2010; Truccolo et al., 2011). Also, to our knowledge, it is not  
103 known if amyloid accumulation affecting EEG power in a broad frequency band is also  
104 entraining single cell activity.

105

106 In recent years, antiepileptic pharmacological treatments to balance altered neuronal  
107 activity as a consequence of amyloid accumulation have become of interest (Cumbo and  
108 Ligori, 2010; Ziyatdinova et al., 2015, 2011). An acute dose of levetiracetam reduces  
109 abnormal EEG spiking activity in the cortex and the hippocampus of an AD mouse model for  
110 18 hours after administration (Sanchez et al., 2012). Notably, sub-chronic treatment with  
111 levetiracetam has been shown to compensate abnormal hypoactivation in the entorhinal  
112 cortex in people with amnesic mild cognitive impairment (aMCI) while simultaneously  
113 improving working memory performance (Bakker et al., 2012). Currently, this treatment is  
114 under clinical testing although the basic mechanisms of action of levetiracetam in AD  
115 patients are not well understood (Bakker et al., 2015). In animal models overexpressing  
116 amyloid protein, acute levetiracetam treatment reduces abnormal spike activity, and chronic  
117 levetiracetam treatment suppresses hippocampal remodeling, behavioral abnormalities,  
118 synaptic dysfunction, and deficits in hippocampal dependent learning and memory (Sanchez  
119 et al., 2012). However, levetiracetam has multiple plausible molecular targets including  
120 voltage-gated ion currents, synaptic vesicle proteins and the glutaminergic system (Surges et  
121 al., 2008), and it is not known which ones are relevant for alleviating AD symptoms.

122

123 Current data, however, provide little information about the dynamics of neuronal ensembles  
124 that give rise to LFP phenomena, excitatory/inhibitory imbalances as a consequence of  
125 amyloid pathology, or on compensatory effects of drugs such as levetiracetam. To  
126 investigate these questions, we recorded both LFP and single cell activity in 4 head-fixed  
127 APP/PS1 mice and 3 wildtype controls and analyzed the effect of acute levetiracetam  
128 treatment. We found that while LFP oscillations showed a power increase in the theta and  
129 beta frequency range as previously reported, frontal cortex pyramidal cell firing rates were  
130 significantly reduced in APP/PS1 mice. At the same time, the sparsely firing pyramidal cells  
131 phase-locked more strongly to the ongoing theta rhythm, Treatment of APP/PS1 mice with  
132 levetiracetam specifically elevated pyramidal cell firing rates and uncoupled pyramidal cells  
133 and interneurons as shown by decreased pair-wise correlations.

134

135 In summary, our results indicate that reduced firing rates of cortical pyramidal cells emerge  
136 as a symptom of amyloid pathology and that treatment with levetiracetam might be a viable  
137 approach to reverse this abnormal activity.

138

## 139 *2. Material and Methods*

### 140 *2.1 Animals*

141

142 For the present study, we used 4 male APP<sub>swe</sub>/PS1<sub>dE9</sub> (APP/PS1) transgenic mice (tg) and 3  
143 age-matched wild type (wt) littermates (all animals underwent the full experiment). The  
144 APP/PS1 founder mice were originally obtained from John Hopkins University, Baltimore,  
145 MD, USA (D. Borchelt and J. Jankowsky, Department of Pathology) and a colony was first  
146 established at the University of Kuopio, Finland. Thereafter a colony was bred at the Central  
147 Animal Facility at Radboud University Medical Center, The Netherlands. The mice were  
148 created by co-injection of chimeric mouse/human A $\beta$ PP<sub>swe</sub> (mouse A $\beta$ PP695 harbouring a  
149 human A $\beta$  domain and mutations K595N and M596L linked to Swedish familial AD  
150 pedigrees) and human PS1-dE9 (deletion of exon 9) vectors controlled by independent  
151 mouse prion protein promoter elements. The two transfected genes co-integrate and co-  
152 segregate as a single locus (Jankowsky et al., 2001). This line was originally maintained on a  
153 hybrid background by backcrossing to C3HeJ×C57BL/6J F1 mice (so-called pseudo F2 stage).  
154 For the present work, the breeder mice were backcrossed to C57BL/6J for 15 generations to

155 obtain mice for the current study. The animals were 9 months old at the start of the  
156 experiment when animals still do not express memory decline. Interestingly, these mice also  
157 display frequent epileptic spiking in the cortex but also the hippocampus, similar to the  
158 previous report by Sanchez et al. 2012 but have characteristic abnormal electrophysiological  
159 phenotype (Gureviciene et al., 2019). All animals were group housed until the first surgery  
160 after which they were individually housed to prevent damage to the implants. Throughout  
161 the experiment, the animals received food and water ad libitum and were maintained on a  
162 12-hour light/dark cycle. Recordings were performed during the light period. All experiments  
163 were approved by the Dutch governmental Central Commissie Dierproeven (CCD) (10300)  
164 and conducted in accordance with the ARRIVE guidelines (Kilkenny et al., 2012).

## 165 166 *2.2 Surgical preparation for head-fixed electrophysiological recordings*

167  
168 Animals were anesthetized using isoflurane (0.8 – 1 l/min, 1.5-2 %) and placed in a  
169 stereotaxic frame. At the onset of anesthesia, all mice received subcutaneous injections of  
170 carprofen (5 mg/kg) as well as a subcutaneous lidocaine injection through the scalp. The  
171 animals' temperature was maintained stable for the duration of the surgical procedure using  
172 a heating blanket. The level of anesthesia was checked during operation by pedal reflex. We  
173 exposed the skull and inserted a skull screw over the cerebellum to serve as combined  
174 reference and ground. We then placed a custom made, circular head-plate for head-fixation  
175 evenly on the skull and fixated it with dental cement (Super-Bond C&B, Sun Medical, Shiga,  
176 Japan). A small craniotomy of about 500µm in diameter was drilled over left frontal cortex at  
177 +1.78mm anterior and 0.4 mm lateral to Bregma. The dura mater was left intact and the  
178 craniotomy, as well as the rest of the exposed skull, were directly covered with a silicone  
179 elastomer (Body Double Fast Set – Trial Size, Reynolds Advanced Materials) until the first  
180 recording. All mice were given at least 2 days to recover from the surgery.

## 181 182 *2.3 Electrophysiological recordings in the frontal cortex of head-fixed mice*

183  
184 The head-fixation setup consisted of two rods that were screwed onto either side of the  
185 implanted head-plate and fixated the mice in place on top of a styrofoam ball that  
186 functioned as an air-supported spherical treadmill and allowed us to read out the movement

187 of the animals in a subset of recording sessions. All animals were slowly habituated to head-  
188 fixation by placing them in the setup for 3 sessions of 10 minutes for two days before the  
189 first recording day.

190

191 Two hours before each recording session, we injected the animals with either 200 mg/kg i.p.  
192 levetiracetam, (Sigma-Aldrich, Taufkirchen, Germany), a dose shown to reduce abnormal  
193 hyperactivity EEG effectively, or saline (control) (Sanchez et al., 2012). We alternated these  
194 injections for 4 consecutive days to be able to record two sessions per animal and condition.  
195 However, during 6 of the later sessions, we weren't able to obtain high quality single cell  
196 recordings either due to a systems malfunction or a gradual development of scar tissue  
197 around the recording sites. We excluded these sessions from the analysis. The experimenter  
198 was blind to both the genotype as well as to the type of treatment (levetiracetam or saline)."

199

200 At the start of each recording session, we placed the mice in head-fixation and removed the  
201 silicone elastomer cover to expose the craniotomy over the frontal cortex. We then used a  
202 micromanipulator (Thorlabs, Newton, New Jersey, USA) to acutely insert a 128 channel  
203 silicon probe (IMEC, Leuven, Belgium) first -1.5mm and then -2.5mm into the frontal cortex.  
204 At each depth, we waited about 15 minutes for the tissue to settle. We then performed 10  
205 minutes of broadband recordings.

206

207 Electrophysiological signals were, digitized at 30 kHz using two digitizing headstages  
208 (RHD2164 Amplifier Board, Intan Technologies, Los Angeles, California, USA), filtered  
209 between 1 and 6000 Hz, and acquired with an open-ephys recording system (Siegle et al.,  
210 2017). After each recording session, we retracted the silicon probe and placed a new silicone  
211 cover on the skull before releasing the animals back to their respective home cages.

212

#### 213 *2.4 Histology*

214

215 At the end of the experiment, the animals were deeply anesthetized with pentobarbital  
216 (Nembutal, pentobarbital sodium 60 mg/ml, 65 mg/kg, i.p.) and perfused with 0.1 M  
217 phosphate buffer (pH = 7.4.) followed by 4% paraformaldehyde solution for 9 min at 10  
218 mL/min. The brain was removed and immersion postfixed for 4 h in 4% paraformaldehyde

219 (pH = 7.4) at 4°C. The brains were thereafter stored at 0.1. phosphate buffer (pH = 7.4) at 4°C  
220 until slicing. Coronal sections (thickness 30  $\mu$ m) were cut with a freezing slide microtome.  
221 Every second section containing a track from the recording electrode were stained for the N-  
222 terminal human A $\beta$ -specific antibody W02 (Genetics, Switzerland) to visualize diffuse  
223 amyloid deposits as described previously (Hooijmans et al., 2007) to verify the amyloid  
224 pathology in the transgenic animals (Fig. 1.). Additionally, we performed a cresyl-violet  
225 staining to verify the anterior-posterior coordinates of the recording sites.

226

### 227 *2.5 Data analysis*

228

229 For LFP analysis, we only used the central channel of our recording electrode. We down-  
230 sampled the broadband signal to 2000 Hz and then low-pass filtered below 500 Hz. Time-  
231 frequency analysis was performed via Morlet wavelet convolution based on the fast Fourier  
232 transform (Cohen, 2014). To minimize the effect of movement on our results, we split each  
233 recording session into 4-s bins and focused our subsequent analysis on the 20 bins with the  
234 highest theta power. Significant differences in the power spectra were calculated using a  
235 permutation test at each frequency.

236

237 To identify single units, data were automatically spike sorted with Kilosort (Pachitariu et al.,  
238 2016) (<https://github.com/cortex-lab/Kilosort>) and then manually inspected with the phy  
239 software (<https://github.com/kwikteam/phy>). All following analyses were performed using  
240 custom written MATLAB scripts. As a post-hoc criterion for the quality of our spike sorting,  
241 we computed the auto-correlograms of each putative single unit and only further analyzed  
242 cells with less than 2% of spikes within the physiological refractory period of 2ms.

243

244 For each unit, we then computed the peak-to-peak amplitude of the action potential  
245 waveforms as well as the width at 30% of the negative peak. We fed these values into  
246 Gaussian-mixture model to classify single units into putative interneurons with narrower  
247 spike waveforms and putative pyramidal cells with broader spike waveform (see Fig. 3 for  
248 cut off criteria) (Stark et al., 2013). In contrast to Stark et al., we used the width of the spike  
249 waveform at 30% (instead of 50%) of the negative peak because visual inspection of all spike  
250 waveform indicated a better separation of putative pyramidal and interneuron waveforms

251 closer to the base of the waveforms than in at 50% (see Fig.3 A). In total, we identified 1394  
252 single neurons for further analysis.

253

254 For each unit, we computed the mean firing rate over the 10-min recording sessions and  
255 performed a 3-factorial ANOVA with neuron type, genotype and drug condition as  
256 independent variables, followed by post-hoc t-tests whenever justified by significant main or  
257 interaction effects.

258

259 Additionally, we computed the spike-time cross-correlations between all simultaneously  
260 recorded neurons using the binned spike trains (5ms bins, `corrcoef` function, MATLAB). We  
261 then performed a 3-factorial ANOVA with neuron type (in this case pyramidal-pyramidal,  
262 interneuron-interneuron and pyramidal-interneuron), genotype and drug condition as  
263 independent variables, followed by post-hoc t-tests whenever justified by significant main or  
264 interaction effects. (Moore et al., 1966; Perkel et al., 1967a, 1967b). For theta and beta  
265 phase locking analysis, we first filtered the raw signal between 4-12 Hz and 12-30 Hz  
266 respectively using a zero-lag band-pass filter (`filtfilt` function, MATLAB) and then extracted  
267 the phase angles using the Hilbert transform (`hilbert` function and `angle` function, MATLAB).  
268 For each putative single cell, we extracted the theta and beta phase angles at each spike and  
269 computed the mean resultant length (`circ_r` function, circular statistic toolbox, MATLAB). In  
270 order to determine if spikes were non- uniformly distributed across different phases of the  
271 ongoing oscillations, we computed the Rayleigh test for circular uniformity of the spike-  
272 phase angles for every cell (`circ_rtest` function, circular statistic toolbox, MATLAB).

273

### 274 3. Results

#### 275 3.1 Increased LFP power in 6-26 Hz band in APP/PS1 mice

276

277 We recorded both local field potential as well as single cell activity with a 128-channel silicon  
278 probe in the frontal cortex of 9-month-old awake, head-fixed APP/PS1 mice and wild type  
279 littermate controls (Fig. 1). We found increased theta and beta LFP power between 6 and 26  
280 Hz in the frontal cortex neurons of APP/PS1 mice (saline injected APP/PS1 n=4 mice, 6

281 sessions; saline injected WT n=3 mice, 4 sessions; permutation test at each frequency  
282  $p < 0.05$ ) (Fig. 2.).

283

### 284 *3.2 Reduced single cell firing rates in the frontal cortex of APP/PS1 mice*

285

286 To test how increased LFP power in the theta and beta frequencies relate to the firing rates  
287 of individual neurons, we performed single cell recordings from the frontal cortex of  
288 APP/PS1 mice. Surprisingly, we found that APP/PS1 mice showed overall reduced firing rates  
289 compared to wildtype controls (n= 422 APP/PS1, n= 255 wt;  $t$ -test,  $p = 0.01$ ).

290

291 To further investigate whether this effect was specific to a certain neuron type, we classified  
292 the recorded single cells as either putative pyramidal cells or interneurons according to their  
293 action potential waveform (Fig. 3 A & B) (Stark et al., 2013). This analysis revealed that the  
294 reduction of firing rates in APP/PS1 mice was statistically significant only for putative  
295 pyramidal cells (ANOVA genotype-neurontype interaction  $F(1,1427)=5.99$ ,  $p=0.01$ ; post hoc  
296  $t$ -test for APP/PS1 (n=372) vs WT pyramidal cells (n=219),  $p=0.006$ , ~21% reduction in mean  
297 firing rates) while interneurons were not significantly affected (post hoc  $t$ -test for APP/PS1  
298 (n=50) vs WT (n=36) interneurons,  $p=.7$ , ~7% decrease in mean firing rates (Fig. 3 C & D).

299

### 300 *3.3 Increased theta and beta phase locking of pyramidal cells in APP/PS1 mice*

301

302 Our analysis of LFP and single cell activity in APP/PS1 mice points towards the non-trivial  
303 relationship between increased local field potential oscillations in the theta and beta range  
304 and the underlying single cell firing rates. To shed light on this issue, we made use of our  
305 simultaneous LFP and unit recordings and analyzed the entrainment of putative pyramidal  
306 cells to the predominant ongoing LFP oscillation in the 4-12 Hz theta and 12-30 Hz beta  
307 range. To this end, we filtered the raw LFP signal between 4-12 Hz and 12-30 Hz,  
308 respectively, and then computed the phase angles using the Hilbert transform. For each  
309 putative single cell, we extracted the theta and beta phase angles for each spike and  
310 computed the mean resultant length. We found that the overall more sparsely firing  
311 pyramidal cells in APP/PS1 mice were significantly more phase-locked to the ongoing theta  
312 and beta oscillation than in wild type controls and clustered around the rising phase of the

313 theta oscillation (theta: Wilcoxon Rank sum test,  $p < 0.001$  (Fig. 4A and 4B.); beta: Wilcoxon  
314 Rank sum test,  $p < 0.001$  (Fig. 4C.);  $n = 227$  (WT/Pyr);  $n = 386$  (APP/PS1/Pyr)). Phase locking in  
315 the gamma range between 30-100 Hz was not significantly affected (gamma: Wilcoxon Rank  
316 sum test,  $p = 0.75$ , Fig. 4D.).

317

318 *3.4 Levetiracetam restores reduced firing rates of single neurons in the frontal cortex*  
319 *of APP/PS1 mice*

320

321 Interestingly, we found that levetiracetam specifically elevated firing rates in frontal cortex  
322 neurons in APP/PS1 mice while firing rates in wildtype animals were not significantly  
323 affected (genotype by drug interaction  $F(1,1427) = 7.79$ ,  $p = 0.005$ ; post hoc  $t$ -test for APP/PS1  
324 cells + lev ( $n = 365$ ) vs APP/PS1 cells + sal ( $n = 431$ ),  $p < 0.001$ ) Importantly, classifying cells into  
325 putative pyramidal cells and interneurons according to their action potential waveforms  
326 revealed that this effect was specific for pyramidal cells (neuron type by drug interaction  
327  $F(1,1427) = 3.91$ ,  $p = 0.048$ ; post hoc  $t$ -test for APP/PS1 pyramidal cells + lev ( $n = 326$ ) vs  
328 APP/PS1 pyramidal cells + sal ( $n = 386$ ),  $p = 0.001$  (Fig. 5 A & B)). We did not find any effect of  
329 levetiracetam on average firing rates on either pyramidal cells or interneurons in wildtype  
330 animals ( $t$ -test for WT + lev ( $n = 370$ ) vs WT + sal ( $n = 262$ ),  $p = 0.85$ ) (Fig. 5 A).

331

332 *3.5 Levetiracetam uncouples pyramidal cells and interneurons in APP/PS1 mice*

333

334 Levetiracetam has been shown to suppress vesicle release (De Smedt et al., 2007; Surges et  
335 al., 2008; Vogl et al., 2012). Therefore, increased firing rates of pyramidal cells in APP/PS1  
336 after treatment with levetiracetam seems more likely to be the result of reduced inhibition  
337 rather than a direct stimulating effect on pyramidal cells. To test this hypothesis, we  
338 analyzed the pair-wise correlations of all simultaneously recorded single cells in APP/PS1  
339 mice (Fig. 5 C & D). In line with its overall positive effect on single cell firing rates,  
340 levetiracetam significantly increased pair-wise pyramidal cell correlations in APP/PS1 mice  
341 (Fig. 5 D). In addition, we specifically analyzed correlations between cell pairs that consisted  
342 of one pyramidal cell and one interneuron in order to clarify the effect on levetiracetam on  
343 the interactions between these cell-types. We found that levetiracetam significantly reduces  
344 pyramidal-interneuron correlations in APP/PS1 mice (Fig. 5 D) (three-way interaction

345 between genotype, neuron type and drug  $F(3,50291)=.643$ ,  $p=0.002$ ; post hoc  $t$ -test for  
346 APP/PS1 pyramidal cells + lev ( $n=9751$ ) vs APP/PS1 pyramidal cells + Sal ( $n=14724$ ),  $p<0.001$ ;  
347 APP/PS1 interneurons + lev ( $n=93$ ) vs APP/PS1 interneurons + sal ( $n=165$ ),  $p<0.001$ ; APP/PS1  
348 pyramidal/interneuron + lev ( $n=1080$ ) vs APP/PS1 pyramidal/interneurons + sal ( $n=1260$ ),  $p<$   
349  $0.001$  ).

350

#### 351 4. Discussion

352

353 Amyloid pathology has been shown to influence the balance between inhibition and  
354 excitation at the level of individual cells and synapses in vitro by modulating both  
355 glutamatergic as well as GABAergic neurotransmission at different stages during disease  
356 progression (Busche et al., 2012; Minkeviciene et al., 2009; Palop et al., 2007; Zott et al.,  
357 2019). Similarly, at the network level, the power of cortical LFP oscillations has previously  
358 been reported to be increased in mouse models of Alzheimer's disease and this increase in  
359 LFP power has been thought to reflect an impairment in the balance of cortical inhibition  
360 and excitation in these animals (Gurevicius et al., 2013; Jin et al., 2018). However, only very  
361 few studies have reported recordings from single neurons in awake behaving animals with  
362 amyloid pathology (Cacucci et al., 2008; Jun et al., 2019). Our understanding of how exactly  
363 changes at excitatory and inhibitory synapses translate into pathologically changed network  
364 activity that can be detected with intracranial LFP or EEG recordings has therefore been very  
365 limited.

366

367 In this context, our data obtained from simultaneous single cell and LFP recordings from the  
368 frontal cortex of 9-month-old amyloid expressing APP/PS1 mice has revealed some  
369 unexpected new insights. In line with previous studies, we found that LFP power was  
370 increased in 9-month-old APP/PS1 mice in the theta and beta frequency bands between 6  
371 and 26 Hz (Gurevicius et al., 2013; Jin et al., 2018). However, our simultaneous recordings of  
372 single cell activity and LFP allowed us to go one step further and analyze single cell firing  
373 rates as well as the precise temporal relationship between action potential firing of  
374 individual cortical neurons and the ongoing LFP oscillations.

375

376 Our data suggest that increased LFP power is likely linked to more synchronized spiking of  
377 cortical neurons instead of increased overall levels of excitability that had previously been  
378 postulated (Gurevicius et al., 2013; Palop and Mucke, 2016). In fact, we found that individual  
379 pyramidal cells in APP/PS1 mice have significantly reduced firing rates compared to wildtype  
380 controls but phase-lock their activity more strongly to the ongoing LFP oscillations in the  
381 beta and theta frequency bands. This overall suppressive effect on firing rates was a surprise  
382 to us because several well established lines of evidence have previously shown that one of  
383 the primary effects of soluble amyloid beta in APP/PS1 mice is an increase in excitation on  
384 the level of individual cells (Minkeviciene et al., 2009). On the single cell level, the amyloid  
385 beta protein was shown to directly increase the excitability of cortical pyramidal cells, and  
386 cortical cells near amyloid plaques were shown to be hyperactive in anaesthetized animals  
387 (Busche et al., 2008; Minkeviciene et al., 2009). However, previous evidence also suggests  
388 that at the network level, likely as a response to this direct excitation caused by amyloid  
389 beta, hippocampal circuits seem to develop a secondary compensatory mechanism which is  
390 characterized by chronically elevated inhibition (Palop et al., 2007). We hypothesis that a  
391 similar principle could apply to cortical circuits in APP/PS1 mice.

392  
393 In support of this view, it has been found that many cortical neurons in anaesthetized AD  
394 mice that are further away from plaques have reduced firing rates. Blocking GABAergic  
395 inhibition with the GABA A receptor antagonist gabazine drastically increases the firing rates  
396 of these neurons (Busche et al., 2008). Furthermore, it has been found that  
397 immunoreactivity against GABA<sub>A</sub> receptor subunit  $\alpha 1$  is significantly elevated in APP/PS1  
398 mice suggesting an increase in postsynaptic inhibition in these animals (Yoshiike et al., 2008).  
399 Finally, the increased likelihood of epileptic seizures in mouse models and patients with AD  
400 has previously been interpreted as a sign for increased cortical excitation instead of  
401 inhibition, however, there is also evidence suggesting that GABA<sub>A</sub> mediated tonic inhibition  
402 can be increased in typical absence epilepsy (Cope et al., 2009; Palop and Mucke, 2016).  
403 Given these multiple factors that influence single cell activity in AD mouse models, a more  
404 detailed electrophysiological characterization, ideally across multiple time-points during  
405 pathology progression, different brain regions and with a higher subject count to account for  
406 inter-animal differences seems ultimately necessary.

407

408 This is particularly relevant because our finding that APP/PS1 mice have overall reduced  
409 firing rates of individual cortical pyramidal cells could have important consequences for  
410 potential therapeutic strategies. To shed light on this issue, we combined single cell  
411 recordings in APP/PS1 mice and treatment with the antiepileptic drug levetiracetam which  
412 has been shown to have various positive effects on Alzheimer's disease pathology and which  
413 has previously been hypothesized to exert these positive effects by reducing neuronal  
414 activity (Bakker et al., 2012; Palop and Mucke, 2016; Sanchez et al., 2012). However, we  
415 found that the mechanisms by which levetiracetam exerts its positive effects during the  
416 treatment of epilepsy and Alzheimer's disease might be more complicated. This likely  
417 includes both reducing pathologically high inhibition during the non-epileptic state in  
418 Alzheimer's disease and reducing aberrant excitation only if and when seizures occur. We  
419 revealed that contrary to the idea that levetiracetam exerts its positive effect in Alzheimer's  
420 disease by reducing excitability, treatment of APP/PS1 mice with levetiracetam in fact leads  
421 to increased firing rates of cortical pyramidal cells. Levetiracetam is known to interact with  
422 the synaptic vesicle protein SV2a which is found in both excitatory and inhibitory synapses  
423 regulating neurotransmitter release (Vogl et al., 2012). Notably, disruption of SV2a function  
424 has been shown to reduce GABA release from inhibitory synapses (Crowder et al., 1999). In  
425 line with these findings, we show that levetiracetam treatment leads to an uncoupling of  
426 inhibitory interneurons and pyramidal cells in APP/PS1 mice as well as to increased firing of  
427 pyramidal cells without affecting interneuron firing rates.

428

429 An important question that arises from this interpretation is that if levetiracetam increases  
430 excitation by lifting inhibition, why does it not result in an increase in seizures but instead  
431 acts as an effective antiepileptic agent? One possible explanation for this is the finding that  
432 levetiracetam acts on both inhibitory and excitatory synapses and that it has been shown to  
433 reduce excitatory transmitter release at glutamatergic synapses in an activity dependent  
434 manner (Yang et al., 2007). Specifically, it was found that at excitatory synapses  
435 levetiracetam reduces the size of repeated excitatory postsynaptic potentials but only during  
436 high frequency stimulation (Meehan et al., 2011; Yang et al., 2007). This frequency  
437 dependency is likely to be the key to the positive effects of levetiracetam which seems to  
438 have relatively little influence on the excitatory transmission during normal, physiological

439 levels of brain activity but has the potential to successfully reduces aberrant firing in a  
440 frequency dependent manner during developing seizures.

441

442 However, future studies, combining simultaneous single cell recordings and levetiracetam  
443 treatment during behavioural testing in amyloid protein expressing mice, will be necessary  
444 to conclusively clarify if levetiracetam exerts its positive influence on cognitive function in  
445 mouse models and patients with Alzheimer's disease primarily through lifting inhibition or  
446 though blocking seizure activity.

447

448

#### 449 *Acknowledgements*

450 We thank Prof. Heikki Tanila for helpful comments on the manuscript and Jos Dederen and  
451 Vivienne Verweij for excellent technical support. The study was supported by the Säätiöiden  
452 post doc -pooli (The Finnish Cultural Foundation) to Dr. Arto Lipponen. Silicon probes were  
453 manufactured by IMEC (Leuven, Belgium) with funding from the European Union's Seventh  
454 Framework Programme (FP7/2007-2013) under grant agreement nr. 600925 (NeuroSeeker).

455

456

457

458

459

460

461

462

463

464

465

466

467

468

469

470

471

472 *References*

- 473 Bakker, A., Albert, M.S., Krauss, G., Speck, C.L., Gallagher, M., 2015. Response of the medial  
474 temporal lobe network in amnesic mild cognitive impairment to therapeutic  
475 intervention assessed by fMRI and memory task performance. *Neuroimage Clin* 7,  
476 688–698. <https://doi.org/10.1016/j.nicl.2015.02.009>
- 477 Bakker, A., Krauss, G.L., Albert, M.S., Speck, C.L., Jones, L.R., Stark, C.E., Yassa, M.A., Bassett,  
478 S.S., Shelton, A.L., Gallagher, M., 2012. Reduction of hippocampal hyperactivity  
479 improves cognition in amnesic mild cognitive impairment. *Neuron* 74, 467–474.  
480 <https://doi.org/10.1016/j.neuron.2012.03.023>
- 481 Busche, M.A., Chen, X., Henning, H.A., Reichwald, J., Staufenbiel, M., Sakmann, B., Konnerth,  
482 A., 2012. Critical role of soluble amyloid- $\beta$  for early hippocampal hyperactivity in a  
483 mouse model of Alzheimer's disease. *Proc. Natl. Acad. Sci. U.S.A.* 109, 8740–8745.  
484 <https://doi.org/10.1073/pnas.1206171109>
- 485 Busche, M.A., Eichhoff, G., Adelsberger, H., Abramowski, D., Wiederhold, K.-H., Haass, C.,  
486 Staufenbiel, M., Konnerth, A., Garaschuk, O., 2008. Clusters of hyperactive neurons  
487 near amyloid plaques in a mouse model of Alzheimer's disease. *Science* 321, 1686–  
488 1689. <https://doi.org/10.1126/science.1162844>
- 489 Busche, M.A., Konnerth, A., 2015. Neuronal hyperactivity--A key defect in Alzheimer's  
490 disease? *Bioessays* 37, 624–632. <https://doi.org/10.1002/bies.201500004>
- 491 Cacucci, F., Yi, M., Wills, T.J., Chapman, P., O'Keefe, J., 2008. Place cell firing correlates with  
492 memory deficits and amyloid plaque burden in Tg2576 Alzheimer mouse model.  
493 *Proc. Natl. Acad. Sci. U.S.A.* 105, 7863–7868.  
494 <https://doi.org/10.1073/pnas.0802908105>
- 495 Cohen, M.X., 2014. Analyzing neural time series data: theory and practice, *Issues in clinical*  
496 *and cognitive neuropsychology*. The MIT Press, Cambridge, Massachusetts.
- 497 Cope, D.W., Di Giovanni, G., Fyson, S.J., Orbán, G., Errington, A.C., Lorincz, M.L., Gould, T.M.,  
498 Carter, D.A., Crunelli, V., 2009. Enhanced tonic GABA inhibition in typical absence  
499 epilepsy. *Nat. Med.* 15, 1392–1398. <https://doi.org/10.1038/nm.2058>
- 500 Crowder, K.M., Gunther, J.M., Jones, T.A., Hale, B.D., Zhang, H.Z., Peterson, M.R., Scheller,  
501 R.H., Chavkin, C., Bajjalieh, S.M., 1999. Abnormal neurotransmission in mice lacking  
502 synaptic vesicle protein 2A (SV2A). *Proc. Natl. Acad. Sci. U.S.A.* 96, 15268–15273.  
503 <https://doi.org/10.1073/pnas.96.26.15268>
- 504 Cumbo, E., Lorigi, L.D., 2010. Levetiracetam, lamotrigine, and phenobarbital in patients with  
505 epileptic seizures and Alzheimer's disease. *Epilepsy Behav* 17, 461–466.  
506 <https://doi.org/10.1016/j.yebeh.2010.01.015>
- 507 De Smedt, T., Raedt, R., Vonck, K., Boon, P., 2007. Levetiracetam: the profile of a novel  
508 anticonvulsant drug-part I: preclinical data. *CNS Drug Rev* 13, 43–56.  
509 <https://doi.org/10.1111/j.1527-3458.2007.00004.x>
- 510 Goutagny, R., Gu, N., Cavanagh, C., Jackson, J., Chabot, J.-G., Quirion, R., Krantic, S., Williams,  
511 S., 2013. Alterations in hippocampal network oscillations and theta-gamma coupling  
512 arise before A $\beta$  overproduction in a mouse model of Alzheimer's disease. *Eur. J.*  
513 *Neurosci.* 37, 1896–1902. <https://doi.org/10.1111/ejn.12233>
- 514 Gureviciene, I., Ishchenko, I., Ziyatdinova, S., Jin, N., Lipponen, A., Gurevicius, K., Tanila, H.,  
515 2019. Characterization of Epileptic Spiking Associated With Brain Amyloidosis in  
516 APP/PS1 Mice. *Front Neurol* 10, 1151. <https://doi.org/10.3389/fneur.2019.01151>

- 517 Gurevicius, K., Lipponen, A., Tanila, H., 2013. Increased cortical and thalamic excitability in  
518 freely moving APP<sup>swe</sup>/PS1<sup>dE9</sup> mice modeling epileptic activity associated with  
519 Alzheimer's disease. *Cereb. Cortex* 23, 1148–1158.  
520 <https://doi.org/10.1093/cercor/bhs105>
- 521 Hardy, J., Selkoe, D.J., 2002. The amyloid hypothesis of Alzheimer's disease: progress and  
522 problems on the road to therapeutics. *Science* 297, 353–356.  
523 <https://doi.org/10.1126/science.1072994>
- 524 Holmes, C., Boche, D., Wilkinson, D., Yadegarfar, G., Hopkins, V., Bayer, A., Jones, R.W.,  
525 Bullock, R., Love, S., Neal, J.W., Zotova, E., Nicoll, J.A.R., 2008. Long-term effects of  
526 Aβ<sub>42</sub> immunisation in Alzheimer's disease: follow-up of a randomised, placebo-  
527 controlled phase I trial. *Lancet* 372, 216–223. [https://doi.org/10.1016/S0140-](https://doi.org/10.1016/S0140-6736(08)61075-2)  
528 [6736\(08\)61075-2](https://doi.org/10.1016/S0140-6736(08)61075-2)
- 529 Hooijmans, C.R., Graven, C., Dederen, P.J., Tanila, H., van Groen, T., Kiliaan, A.J., 2007.  
530 Amyloid beta deposition is related to decreased glucose transporter-1 levels and  
531 hippocampal atrophy in brains of aged APP/PS1 mice. *Brain Res.* 1181, 93–103.  
532 <https://doi.org/10.1016/j.brainres.2007.08.063>
- 533 Jankowsky, J.L., Slunt, H.H., Ratovitski, T., Jenkins, N.A., Copeland, N.G., Borchelt, D.R., 2001.  
534 Co-expression of multiple transgenes in mouse CNS: a comparison of strategies.  
535 *Biomol. Eng.* 17, 157–165.
- 536 Jin, N., Lipponen, A., Koivisto, H., Gurevicius, K., Tanila, H., 2018. Increased cortical beta  
537 power and spike-wave discharges in middle-aged APP/PS1 mice. *Neurobiol. Aging* 71,  
538 127–141. <https://doi.org/10.1016/j.neurobiolaging.2018.07.009>
- 539 Jiruska, P., de Curtis, M., Jefferys, J.G.R., Schevon, C.A., Schiff, S.J., Schindler, K., 2013.  
540 Synchronization and desynchronization in epilepsy: controversies and hypotheses. *J.*  
541 *Physiol. (Lond.)* 591, 787–797. <https://doi.org/10.1113/jphysiol.2012.239590>
- 542 Joutsa, J., Rinne, J.O., Hermann, B., Karrasch, M., Anttinen, A., Shinnar, S., Sillanpää, M.,  
543 2017. Association Between Childhood-Onset Epilepsy and Amyloid Burden 5 Decades  
544 Later. *JAMA Neurol* 74, 583–590. <https://doi.org/10.1001/jamaneurol.2016.6091>
- 545 Jun, H., Soma, S., Saito, T., Saido, T.C., Igarashi, K.M., 2019. Disrupted remapping of place  
546 cells and grid cells in knock-in model of Alzheimer's disease. *bioRxiv* 815993.  
547 <https://doi.org/10.1101/815993>
- 548 Keller, C.J., Truccolo, W., Gale, J.T., Eskandar, E., Thesen, T., Carlson, C., Devinsky, O.,  
549 Kuzniecky, R., Doyle, W.K., Madsen, J.R., Schomer, D.L., Mehta, A.D., Brown, E.N.,  
550 Hochberg, L.R., Ulbert, I., Halgren, E., Cash, S.S., 2010. Heterogeneous neuronal firing  
551 patterns during interictal epileptiform discharges in the human cortex. *Brain* 133,  
552 1668–1681. <https://doi.org/10.1093/brain/awq112>
- 553 Kellner, V., Menkes-Caspi, N., Beker, S., Stern, E.A., 2014. Amyloid-β alters ongoing neuronal  
554 activity and excitability in the frontal cortex. *Neurobiology of Aging* 35, 1982–1991.  
555 <https://doi.org/10.1016/j.neurobiolaging.2014.04.001>
- 556 Kilkenny, C., Browne, W.J., Cuthill, I.C., Emerson, M., Altman, D.G., 2012. Improving  
557 bioscience research reporting: the ARRIVE guidelines for reporting animal research.  
558 *Osteoarthr. Cartil.* 20, 256–260. <https://doi.org/10.1016/j.joca.2012.02.010>
- 559 Lam, A.D., Deck, G., Goldman, A., Eskandar, E.N., Noebels, J., Cole, A.J., 2017. Silent  
560 hippocampal seizures and spikes identified by foramen ovale electrodes in  
561 Alzheimer's disease. *Nat. Med.* 23, 678–680. <https://doi.org/10.1038/nm.4330>
- 562 Meehan, A.L., Yang, X., McAdams, B.D., Yuan, L., Rothman, S.M., 2011. A new mechanism for  
563 antiepileptic drug action: vesicular entry may mediate the effects of levetiracetam. *J.*  
564 *Neurophysiol.* 106, 1227–1239. <https://doi.org/10.1152/jn.00279.2011>

- 565 Minkeviciene, R., Rheims, S., Dobszay, M.B., Zilberter, M., Hartikainen, J., Fülöp, L., Penke, B.,  
566 Zilberter, Y., Harkany, T., Pitkänen, A., Tanila, H., 2009. Amyloid beta-induced  
567 neuronal hyperexcitability triggers progressive epilepsy. *J. Neurosci.* 29, 3453–3462.  
568 <https://doi.org/10.1523/JNEUROSCI.5215-08.2009>
- 569 Moore, G.P., Perkel, D.H., Segundo, J.P., 1966. Statistical analysis and functional  
570 interpretation of neuronal spike data. *Annu. Rev. Physiol.* 28, 493–522.  
571 <https://doi.org/10.1146/annurev.ph.28.030166.002425>
- 572 Nagy, Z., Esiri, M.M., Jobst, K.A., Morris, J.H., King, E.M.-F., McDonald, B., Litchfield, S., Smith,  
573 A., Barnetson, L., Smith, A.D., 1995. Relative Roles of Plaques and Tangles in the  
574 Dementia of Alzheimer's Disease: Correlations Using Three Sets of Neuropathological  
575 Criteria. *Dementia and Geriatric Cognitive Disorders* 6, 21–31.  
576 <https://doi.org/10.1159/000106918>
- 577 Palop, J.J., Chin, J., Roberson, E.D., Wang, J., Thwin, M.T., Bien-Ly, N., Yoo, J., Ho, K.O., Yu, G.-  
578 Q., Kreitzer, A., Finkbeiner, S., Noebels, J.L., Mucke, L., 2007. Aberrant excitatory  
579 neuronal activity and compensatory remodeling of inhibitory hippocampal circuits in  
580 mouse models of Alzheimer's disease. *Neuron* 55, 697–711.  
581 <https://doi.org/10.1016/j.neuron.2007.07.025>
- 582 Palop, J.J., Mucke, L., 2016. Network abnormalities and interneuron dysfunction in Alzheimer  
583 disease. *Nat. Rev. Neurosci.* 17, 777–792. <https://doi.org/10.1038/nrn.2016.141>
- 584 Pena-Ortega, F., Solis-Cisneros, A., Ordaz, B., Balleza-Tapia, H., Javier Lopez-Guerrero, J.,  
585 2012. Amyloid beta 1-42 inhibits entorhinal cortex activity in the beta-gamma range:  
586 role of GSK-3. *Curr Alzheimer Res* 9, 857–863.
- 587 Perkel, D.H., Gerstein, G.L., Moore, G.P., 1967a. Neuronal spike trains and stochastic point  
588 processes. I. The single spike train. *Biophys. J.* 7, 391–418.  
589 [https://doi.org/10.1016/S0006-3495\(67\)86596-2](https://doi.org/10.1016/S0006-3495(67)86596-2)
- 590 Perkel, D.H., Gerstein, G.L., Moore, G.P., 1967b. Neuronal spike trains and stochastic point  
591 processes. II. Simultaneous spike trains. *Biophys. J.* 7, 419–440.  
592 [https://doi.org/10.1016/S0006-3495\(67\)86597-4](https://doi.org/10.1016/S0006-3495(67)86597-4)
- 593 Sanchez, P.E., Zhu, L., Verret, L., Vossel, K.A., Orr, A.G., Cirrito, J.R., Devidze, N., Ho, K., Yu, G.-  
594 Q., Palop, J.J., Mucke, L., 2012. Levetiracetam suppresses neuronal network  
595 dysfunction and reverses synaptic and cognitive deficits in an Alzheimer's disease  
596 model. *Proc. Natl. Acad. Sci. U.S.A.* 109, E2895-2903.  
597 <https://doi.org/10.1073/pnas.1121081109>
- 598 Schevon, C.A., Weiss, S.A., McKhann, G., Goodman, R.R., Yuste, R., Emerson, R.G., Trevelyan,  
599 A.J., 2012. Evidence of an inhibitory restraint of seizure activity in humans. *Nat*  
600 *Commun* 3, 1060. <https://doi.org/10.1038/ncomms2056>
- 601 Siegle, J.H., López, A.C., Patel, Y.A., Abramov, K., Ohayon, S., Voigts, J., 2017. Open Ephys: an  
602 open-source, plugin-based platform for multichannel electrophysiology. *J Neural Eng*  
603 14, 045003. <https://doi.org/10.1088/1741-2552/aa5eea>
- 604 Stark, E., Eichler, R., Roux, L., Fujisawa, S., Rotstein, H.G., Buzsáki, G., 2013. Inhibition-  
605 induced theta resonance in cortical circuits. *Neuron* 80.  
606 <https://doi.org/10.1016/j.neuron.2013.09.033>
- 607 Surges, R., Volynski, K.E., Walker, M.C., 2008. Is levetiracetam different from other  
608 antiepileptic drugs? Levetiracetam and its cellular mechanism of action in epilepsy  
609 revisited. *Ther Adv Neurol Disord* 1, 13–24.  
610 <https://doi.org/10.1177/1756285608094212>

- 611 Truccolo, W., Donoghue, J.A., Hochberg, L.R., Eskandar, E.N., Madsen, J.R., Anderson, W.S.,  
612 Brown, E.N., Halgren, E., Cash, S.S., 2011. Single-neuron dynamics in human focal  
613 epilepsy. *Nat. Neurosci.* 14, 635–641. <https://doi.org/10.1038/nn.2782>
- 614 Verret, L., Mann, E.O., Hang, G.B., Barth, A.M.I., Cobos, I., Ho, K., Devidze, N., Masliah, E.,  
615 Kreitzer, A.C., Mody, I., Mucke, L., Palop, J.J., 2012. Inhibitory interneuron deficit links  
616 altered network activity and cognitive dysfunction in Alzheimer model. *Cell* 149, 708–  
617 721. <https://doi.org/10.1016/j.cell.2012.02.046>
- 618 Vogl, C., Mochida, S., Wolff, C., Whalley, B.J., Stephens, G.J., 2012. The synaptic vesicle  
619 glycoprotein 2A ligand levetiracetam inhibits presynaptic Ca<sup>2+</sup> channels through an  
620 intracellular pathway. *Mol. Pharmacol.* 82, 199–208.  
621 <https://doi.org/10.1124/mol.111.076687>
- 622 Vossel, K.A., Beagle, A.J., Rabinovici, G.D., Shu, H., Lee, S.E., Naasan, G., Hegde, M., Cornes,  
623 S.B., Henry, M.L., Nelson, A.B., Seeley, W.W., Geschwind, M.D., Gorno-Tempini, M.L.,  
624 Shih, T., Kirsch, H.E., Garcia, P.A., Miller, B.L., Mucke, L., 2013. Seizures and  
625 epileptiform activity in the early stages of Alzheimer disease. *JAMA Neurol* 70, 1158–  
626 1166. <https://doi.org/10.1001/jamaneurol.2013.136>
- 627 Wyler, A.R., Ojemann, G.A., Ward, A.A., 1982. Neurons in human epileptic cortex: correlation  
628 between unit and EEG activity. *Ann. Neurol.* 11, 301–308.  
629 <https://doi.org/10.1002/ana.410110311>
- 630 Yang, X.-F., Weisenfeld, A., Rothman, S.M., 2007. Prolonged exposure to levetiracetam  
631 reveals a presynaptic effect on neurotransmission. *Epilepsia* 48, 1861–1869.  
632 <https://doi.org/10.1111/j.1528-1167.2006.01132.x>
- 633 Yoshiike, Y., Kimura, T., Yamashita, S., Furudate, H., Mizoroki, T., Murayama, M., Takashima,  
634 A., 2008. GABA(A) receptor-mediated acceleration of aging-associated memory  
635 decline in APP/PS1 mice and its pharmacological treatment by picrotoxin. *PLoS ONE*  
636 3, e3029. <https://doi.org/10.1371/journal.pone.0003029>
- 637 Ziyatdinova, S., Gurevicius, K., Kutchiashvili, N., Bolkvadze, T., Nissinen, J., Tanila, H.,  
638 Pitkänen, A., 2011. Spontaneous epileptiform discharges in a mouse model of  
639 Alzheimer's disease are suppressed by antiepileptic drugs that block sodium  
640 channels. *Epilepsy Res.* 94, 75–85. <https://doi.org/10.1016/j.eplepsyres.2011.01.003>
- 641 Ziyatdinova, S., Viswanathan, J., Hiltunen, M., Tanila, H., Pitkänen, A., 2015. Reduction of  
642 epileptiform activity by valproic acid in a mouse model of Alzheimer's disease is not  
643 long-lasting after treatment discontinuation. *Epilepsy Res.* 112, 43–55.  
644 <https://doi.org/10.1016/j.eplepsyres.2015.02.005>
- 645 Zott, B., Simon, M.M., Hong, W., Unger, F., Chen-Engerer, H.-J., Frosch, M.P., Sakmann, B.,  
646 Walsh, D.M., Konnerth, A., 2019. A vicious cycle of  $\beta$  amyloid-dependent neuronal  
647 hyperactivation. *Science* 365, 559–565. <https://doi.org/10.1126/science.aay0198>

648

649

650

651

652

653

654

655  
 656  
 657  
 658  
 659  
 660  
 661  
 662  
 663  
 664  
 665  
 666  
 667  
 668  
 669  
 670  
 671  
 672  
 673  
 674  
 675  
 676  
 677  
 678  
 679  
 680  
 681  
 682  
 683  
 684  
 685  
 686  
 687  
 688  
 689  
 690  
 691  
 692  
 693  
 694  
 695

*Figure legends*

*Figure 1. Representative histological sections from a transgenic APP/PS1 mouse; W02 antibody staining for A $\beta$  deposits revealed plaques in the frontal somatosensory cortex (left) and two reconstructed electrode positions from successive recordings (right) (scale bars: left=100  $\mu$ m, right 200  $\mu$ m).*

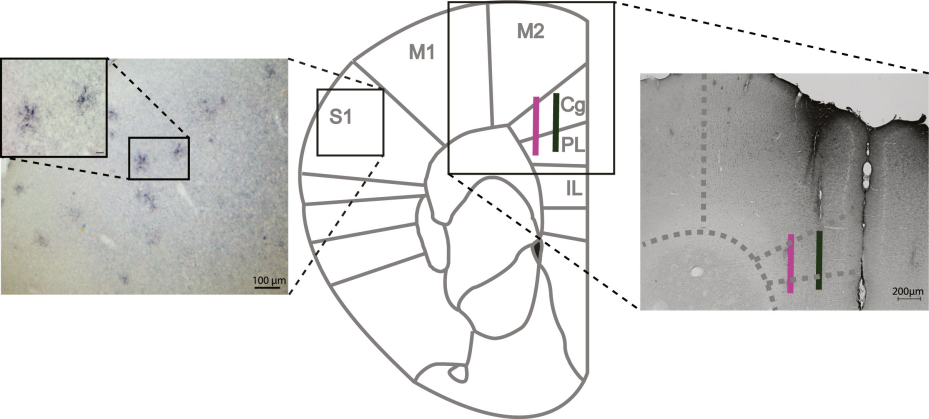
*Figure 2. Increased LFP Power in APP/PS1 mice; Population average power from APP/PS1 mice and wild type controls (APP/PS1 n=4 mice, 6 sessions; WT n=3 mice, 4 Sessions). Black bar indicates significant Power differences from 6-28 Hz (permutation test at each Frequency  $p < 0.05$ ). Shaded areas indicate SEM.*

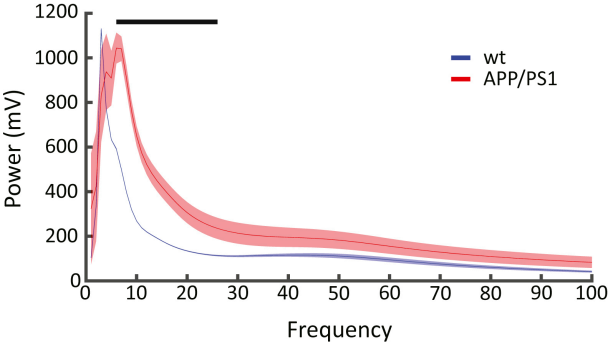
*Figure 3. Decreased pyramidal cell firing rates in APP/PS1 mice A) Average action potential waveforms of all recorded putative pyramidal cells (blue) and interneurons (red) B) Spike width vs. valley to peak ratio of all recorded single cells, color-coded according to Gaussian mixture model classification. C) Average firing rates of putative pyramidal cells and interneurons in saline treated wild-type controls and APP/PS1 mice (n=228 (WT/Pyr); 386 (APP/PS1/Pyr); 35 (WT/Int); 45 (APP/PS1/Int); \*\* indicates  $p < 0.01$ ). Error bars represent SEM. D) Comparison between pyramidal cell firing rates in individual wild-type vs individual APP/PS1 mice (\*\* indicates  $p < 0.01$  between groups (same as in C); Error bars represent SEM).*

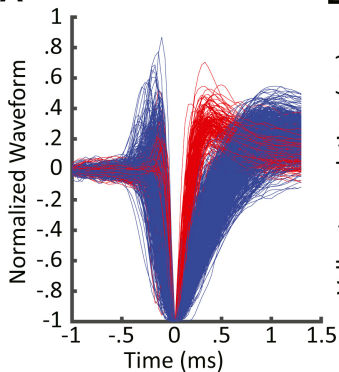
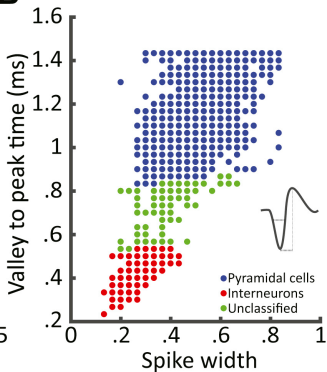
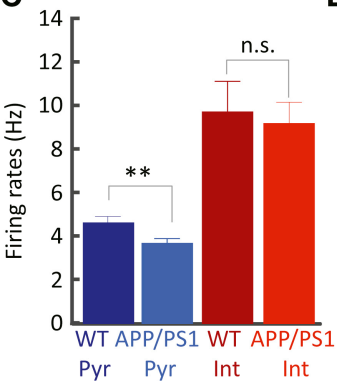
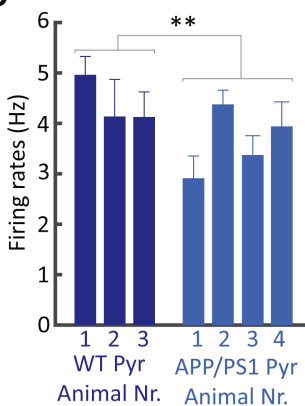
*Figure 4. Theta & beta phase - pyramidal cell spike coherence is increased in APP/PS1 mice. A) Example periods from APP/PS1 (top) and WT (bottom) recording sessions, showing LFP (red), theta (green) and pyramidal cell firing (blue). Note that overall sparser spikes are clusters around theta troughs in APP/PS1 mice. B) APP/PS1 pyramidal cells are significantly more locked to theta (MRL= mean resultant length, \*\*\*indicates  $p < .001$ , n=228 (WT/Pyr); 386 (APP/PS1/Pyr)). Error bars represent SEM (left) Distribution of average firing phase of all significantly modulated WT (blue) and APP/PS1 (red) pyramidal cells (Rayleigh test for circular uniformity) (right). Green line on top indicates Theta phase. C) APP/PS1 pyramidal cells are significantly more locked to the ongoing beta oscillations than pyramidal cells in wild-type controls (MRL= mean resultant length, \*\*\*indicates  $p < .001$ , n=228 (WT/Pyr); 386 (APP/PS1/Pyr)). D) APP/PS1 pyramidal cells are not significantly more locked to the ongoing gamma oscillations than pyramidal cells in wild-type controls (30-100 Hz) ( $p = .75$ ).*

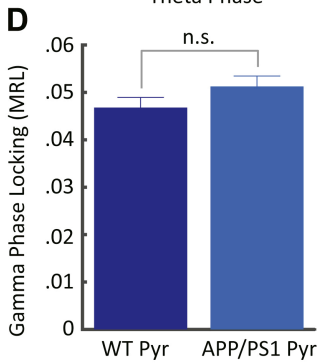
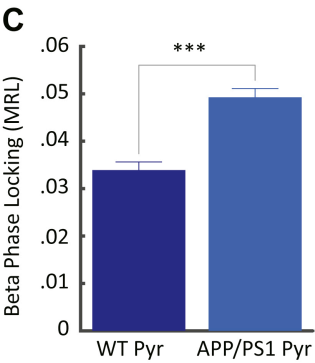
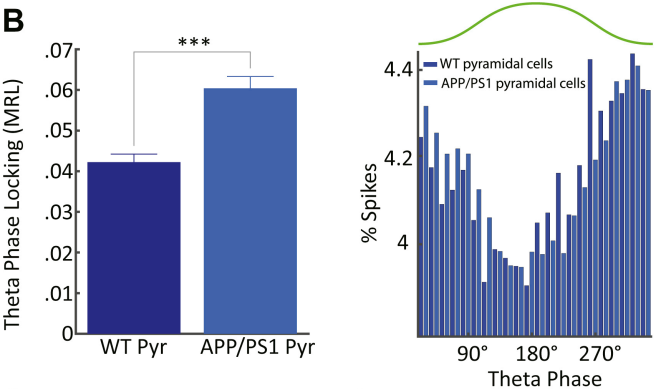
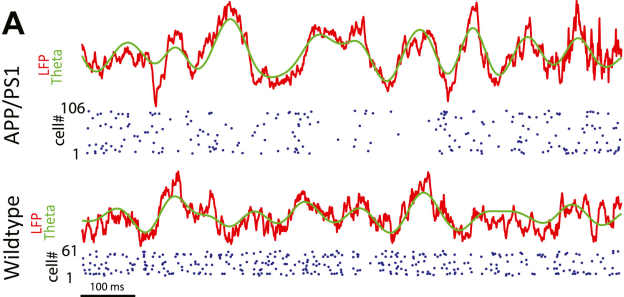
696

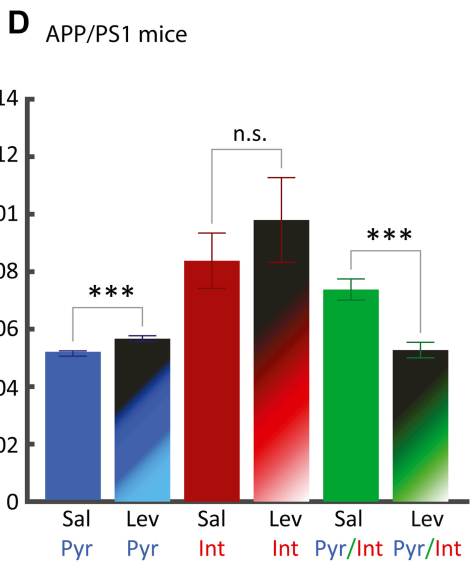
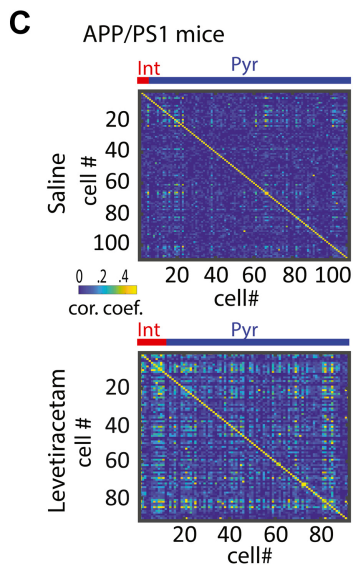
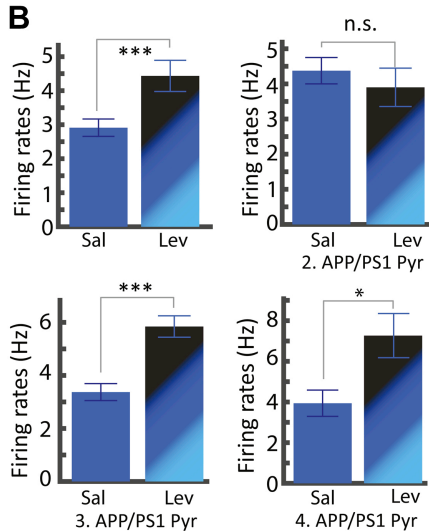
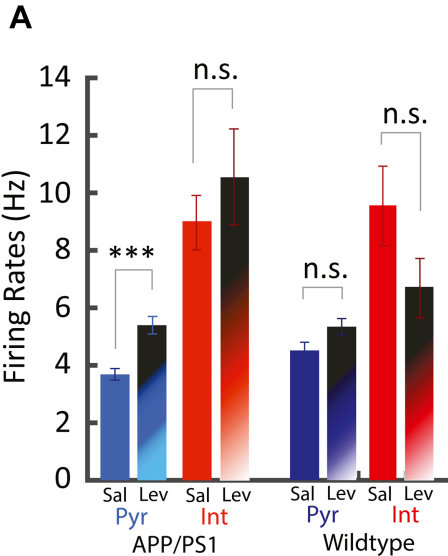
697 *Figure 5. Levetiracetam restores pyramidal cell firing rates in APP/PS1 mice. A) Average firing*  
698 *rates of putative pyramidal cells and interneurons in APP/PS1 mice treated either with saline*  
699 *or levetiracetam injections (n=386 (APP/PS1/Pyr/Sal); 326 (APP/PS1/Pyr/Lev); 45*  
700 *(APP/PS1/Int/Sal); 39 (APP/PS1/Int/Lev ;\*\*\* indicates  $p<0.001$ ; Error bars represent SEM). B)*  
701 *Average firing rates in individual APP/PS1 mice treated with saline or levetiracetam*  
702 *(\*indicates  $p<0.05$ ; \*\*\* indicates  $p<0.001$ ; Error bars represent SEM). C) Example sessions of*  
703 *pairwise correlations of simultaneously recorded neurons from one animal with saline (top)*  
704 *and levetiracetam (bottom) injections. Red and blue bar indicates interneurons and*  
705 *pyramidal cells. D) Average pairwise correlations of all simultaneously recorded pyramidal*  
706 *cells (blue), interneurons (red) and pyramidal – interneuron cell pairs (green) (\*\*\*) indicates*  
707  *$p<0.001$ ; Error bars represent SEM) (right).*





**A****B****C****D**





*Highlights*

- *9 months old APP/PS1 mice exhibit increased theta and beta oscillations in the frontal cortex*
- *Pyramidal cell firing rates are significantly decreased but more phase-locked to ongoing LFP oscillations*
- *Levetiracetam treatment uncouples pyramidal cells and interneurons and elevates pyramidal cell firing rates*

Journal Pre-proof

**Jan L Klee:** Conceptualization, Methodology, Formal analysis, Investigation, Writing – Original Draft, Writing – Review and Editing, Visualization, Project administration.

**Amanda J. Kiliaan:** Conceptualization, Resources, Writing – Original Draft, Writing – Review and Editing.

**Arto Lipponen:** Conceptualization, Methodology, Investigation, Writing – Original Draft, Writing – Review and Editing, Visualization, Supervision, Funding acquisition, Project administration.

**Francesco P. Battaglia:** Conceptualization, Methodology, Resources, Writing – Original Draft, Writing – Review and Editing, Supervision, Funding acquisition

1. The authors report no conflicts of interest. The manuscript is unpublished and not being offered for publication elsewhere.
2. The study was supported by the Säätiöiden post doc -pooli (The Finnish Cultural Foundation) to Dr. Arto Lipponen. Silicon probes were manufactured by IMEC (Leuven, Belgium) with funding from the European Union's Seventh Framework Programme (FP7/2007-2013) under grant agreement nr. 600925 (NeuroSeeker).
3. The manuscript is unpublished and not being offered for publication elsewhere.
4. The manuscript meets the guidelines for ethical conduct and report of research. All experiments were approved by the Dutch governmental Central Commissie Dierproeven (CCD) (10300) and conducted in accordance with the ARRIVE guidelines.
5. All authors have reviewed the contents of the manuscript being submitted, approve of its contents and validate the accuracy of the data.